A Study on the Effect of Ion Irradiation on Metal Oxide Thin Films Coated/Embedded with Noble Metal Nanoparticles for Photoelectrochemical Splitting of Water for Hydrogen Production

A synopsis of the proposed work for the award of the degree

Doctor of Philosophy
In Chemistry

Anuradha Verma

Forwarded By:

Prof. Sahab Dass
Supervisor
Dept. of Chemistry
Dayalbagh Educational Institute

Dr. D. K. Avasthi
Co-Supervisor
Head, Material Science Division
IUAC, New Delhi

Prof. L. D. Khemani
Head, Dept. of Chemistry
Dean, Faculty of Science

DEPARTMENT OF CHEMISTRY
FACULTY OF SCIENCE
DAYALBAGH EDUCATIONAL INSTITUTE
(DEEMED UNIVERSITY)
DAYALBAGH, AGRA-282005
(July, 2013)

1. Introduction

1.1 Need of an Alternative Energy Sources

Supply and demand of energy determine the course of global development in every sphere of human activity. It has been realized that existing sources of energy derived from fossil fuels being limited will not be able to fulfill the increasing demand of future generation. Apart from that, decarburizing our energy sources is also an important issue because their continuous use creates well known hazards which threaten human health and are associated with global climate change, such as greenhouse effect, ozone layer depletion, acid rain and pollution and are posing great danger for our environment and eventually for the life on our planet.

Hydrogen is an extremely valuable chemical commodity as is vital to future of our planet and its people and is emerging as green economy. Use of solar, wind, geothermal and other renewable energy resources and lesser dependence on fossil fuel will lead to the development of "Green" futures[1].

The scientists world over have accelerated the innovations on finding sustainable alternate sources of energy, and research is narrowing down to "zero carbon fuel Hydrogen", which only has the potential to fulfill the need to be a clean, reliable and sustainable energy carrier, satisfying the need of both – the hearth and the wheel. Hydrogen is gaining increasing attention scientifically and is considered one of the most promising energy carriers as it is an efficient and clean energy carrier and has potential to meet the requirements as a clean fuel in the future[2].

1.2 Hydrogen: Promising Future Fuel

In 1671, Robert Boyle produced Hydrogen gas in an experiment with iron and acids. It was recognized as a distinct element by Henry Cavendish in 1766. Hydrogen is omnipresent and has tremendous energy content. It forms the basis of life as it forms water on combination with oxygen, another vital gas[2].

The Hydrogen atom is a simple combination of an electron and a proton. It is perhaps the simplest element known to man and is virtually the basic building block of the universe. The importance of the gas is amazing. Its range of uses includes edible fats & oils on one hand and superconductors & rocket fuel for space ships, on the other[2].

The need of developing hydrogen as a fuel instead of fossil fuel is very pertinent owing to reasons given below[3]:

1. Fossil fuel use lead to climate change due to harmful gases emission associated with them.
2. Fossil fuel deposits are limited.
3. Fossil fuel price is increasing.
4. Fuel should be environmentally safe and renewable.
5. Fuel should be generated from abundantly available natural resources.

Advantages of using hydrogen as a fuel:

1. Hydrogen has high heat of combustion (34.18 kcal/g for H_2 and 10.30 kcal/g for petroleum).
2. Energy Released from hydrogen is 140 kJ/g while that of methane is only 33 kJ/g
3. Energy storage capacity/mole of H_2 is 119 kJ/g while that of oil is 40 kJ/g .
4. **Security of energy supply:** It can be produced from renewable energy sources (e.g. wind, solar, ocean, and biomass)
5. **Air quality and health improvement:** Vehicles fuelled by hydrogen are zero-emission devices. Hydrogen vehicles do not contribute to pollution in the urban areas where the traffic is high
6. **Greenhouse gas reduction:** Hydrogen when burned, only emission is water vapor, no carbon dioxide (CO_2) is produced.
7. **Easy Storage:** Hydrogen is a gas, thus easier to store than electricity.
8. Easy transportation through gas pipelines without any conversions.

Applications of hydrogen include:

1. Powering non-polluting vehicles
2. Domestic heating
3. Fueling aircraft
4. As fuel in fuel cell for electricity

1.3 Hydrogen Generation from Solar Energy

Hydrogen has been produced mainly from methane using steam reforming but is associated with CO_2 emission. Hydrogen production from water electrolysis using the electricity (obtained from the combustion of fossil fuels) is also having the same problem[3].

Sun is the ultimate renewable energy resource which continuously bombards earth with 180,000 TW of radiant power, of this 36000 TW is absorbed by earths land masses. Our society on average consumes nearly 13- 15 TW[1]. In order to avoid the most serious consequences of global climate change and to ensure adequate global energy supply to avoid economic chaos it is estimated that at least 20 TW of carbon free energy (1.5 times the total amount of all forms of energy consumed today globally), in the form of electricity and liquid and gaseous fuels, will be required by 2050[5]. Solar hydrogen production is one technology that can potentially provide a clean, cost effective, and domestically produced energy carrier[4]. Harvesting solar energy for electrolysis of water in a system in which photon energy is converted to electrical energy, which is directly used to split water into hydrogen and oxygen (chemical energy). Thus intermittent solar energy is converted into an inherently more storable form of energy, that of chemical bonds[4].

1.4 Methods of Hydrogen Production

Hydrogen can be produced from fossil fuels, biomass, or water and requires a source of energy, i.e., thermal (heat), electrolytic (electricity), or photolytic (light) energy. Researchers are involved in developing technologies to produce hydrogen in economical and environmentally friendly ways.

But overall challenge for hydrogen production is its cost reduction.

Hydrogen production technologies generally fall in three categories

1. Thermal Processes

- ✓ Natural gas reforming (Nonrenewable resource, CO_2 emissions)
- ✓ Gasification - Hydrogen from coal (CO_2 emissions)

2. Electrolytic Processes

   Production may require more energy than released, CO_2 emissions if coal is energy source

3. Photolytic Processes

- ✓ Photobiological Water Splitting
- ✓ Photoelectrochemical Water Splitting

1.5 Photoelectrochemical Water Splitting for Hydrogen Production

PEC technology for splitting of water into hydrogen and oxygen by the direct use of sunlight is an ideal and promising technology for hydrogen production because of several reasons[3]:

1. PEC technology is based on solar energy and water both are renewable resource.
2. PEC technology is environmentally safe, with no undesirable byproducts.
3. PEC technology may be used on both large and small scales.
4. PEC technology is relatively uncomplicated.

This method of hydrogen production integrates solar energy collection and water electrolysis in a single photocell. When a semiconductor with the right set of properties is immersed in an aqueous electrolyte and irradiated with sunlight, the photon energy is converted to electrical energy, which is directly used to split water into hydrogen and oxygen (chemical energy). Thus intermittent solar energy is converted into an inherently more storable form of energy, that of chemical bonds.

The efficient photoelectrochemical cell converts water into hydrogen and oxygen using sunlight in a two electrode system; semiconductor (possessing either p-or n-type conductivity) as working

electrode and platinum (Pt) as counter electrode (as shown in Fig. 1). However in most measurements reference electrode is also employed to investigate half reactions in the PEC cell. There are three options for arrangement of electrodes in PEC assembly[3]:

1. Photo-anode- n-type semiconductor (O_2)
   Cathode- metal (H_2)

2. Photo-anode- n-type semiconductor (O_2)
   Photo-cathode- p-type semiconductor (H_2)

3. Photo-cathode- p-type semiconductor (H_2)
   Anode- metal (O_2)

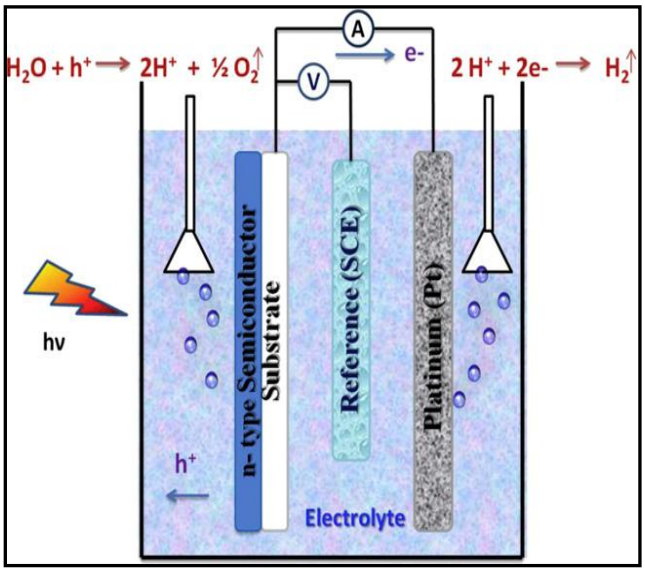

Fig. 1. Schematic diagram of photoelectrochemical cell consisting of n-type semiconductor photoanode, reference (SCE) and metal cathode for water splitting[7].

The aim of *artificial photosynthesis* is the light-driven splitting of water into H_2 and O_2, is a thermodynamically uphill reaction ($\Delta G \approx 237.2$ kJ/mol)

$$2H_2O \longrightarrow O_2 + 2H_2 \text{ (Light)}$$

The photoelectrochemical (PEC) path to water splitting involves separating the oxidation and reduction processes into half-cell reactions. The negative $\Delta E°$ indicates that water splitting is not a thermodynamically spontaneous process.

For the reaction to proceed 1.23 V must be provided externally.

Oxidation:

$$2H_2O \longrightarrow O_2 + 4H^+ + 4e^-$$
$$E° = 1.23 \text{ V } \textit{vs.} \text{ SHE}$$

Reduction:

$$2H^+ + 2e^- \longrightarrow H_2$$
$$E° = 0.00 \text{ V } vs. \text{ SHE}$$

Overall:

$$2H_2O \longrightarrow O_2 + 2H_2$$
$$\Delta E° = -1.23 \text{ V}$$

But energy losses (- 0.8 eV) caused by the recombination of the photogenerated charge carriers, resistance of the electrodes and electrical connections and voltage losses at the contacts etc., voltage of 1.6-2.0 eV is needed for spontaneous water splitting[7].

Upon illumination with photons having energy equal or larger than the band gap (E_g) of the semiconductor, electron-hole pairs are generated. In case of n-type semiconductor electrode, the holes react with water molecules at semiconductor surface resulting into O_2 formation whereas electrons travel through substrate and then to external circuit and are transported to the counter electrode where they reduce H^+ into H_2. On the contrary, p-type semiconductor electrode produces H_2 and O_2 at semiconductor electrode and at counter electrode respectively.

Step1. Absorption of light near the surface of the semiconductor creates electron-hole pairs.

Step2. Holes (minority carriers) drift to the surface of the semiconductor (the photo anode) where they react with water to produce oxygen:

$$2h^+ + H_2O \longrightarrow ½\ O_2\ (g) + 2H^+$$

Step3. Electrons (majority carriers) are conducted to a metal electrode (typically Pt) where they combine with H^+ ions in the electrolyte solution to make H_2

$$2e^- + 2H^+ \longrightarrow H_2\ (g)$$

Step4. Transport of H^+ from the anode to the cathode through the electrolyte completes the electrochemical circuit. The overall reaction:

$$2h\nu + H_2O \longrightarrow H_2\ (g) + ½\ O_2\ (g)$$

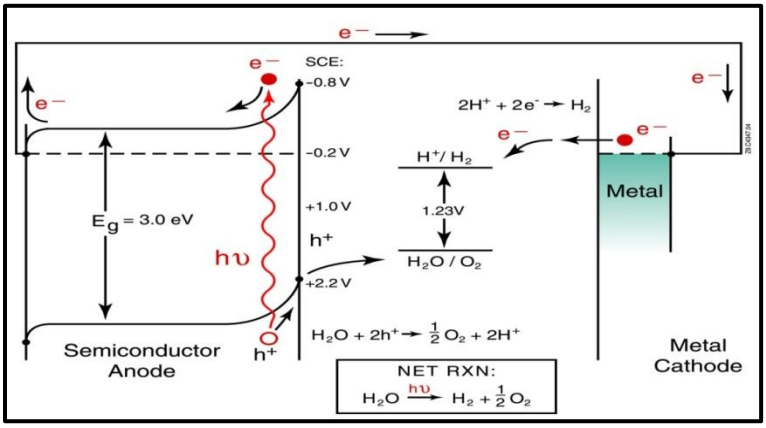

Fig.2. Working Principle of Photoelectrochemical Cell for Water Splitting

1.6 Semiconductor Electrode: Heart of PEC System

Photoelectrochemical hydrogen production cell involves different arrangement of working electrode, counter electrode and reference electrode. Semiconductor electrode depending upon its nature (n/p- type) may serve as working or counter electrode. Semiconductor is photoactive and is the heart of PEC cell since it absorbs light near its surface and generates electron-hole pairs. Depending on the nature of semiconductor electrons and hole migrate to the respective electrode to generate H_2 and O_2.

Desired properties of photoelectrodes are[7]:

1. Optical function required to obtain maximal absorption of solar energy
2. Catalytic function required for water decomposition i.e. O_2 (or H_2) evolution.
3. Band gap -1.6–2.0 eV
4. Corrosion resistance
5. Band edges must straddle H_2O redox potentials
6. Long life time of charge carriers

Performance Criteria for Photoelectrode are[7]:

1. Long-term stability in aqueous electrolyte
2. Durability > 2000h
3. Low cost of manufacturing
4. Ease of maintenance
5. Conversion efficiency, solar to hydrogen (STH) > 10%

The search for a semiconductor with all above desired characteristics is still a challenge before the scientific communities at large and world over various groups are working to develop such a semiconductor.

High band gap materials show poor harvesting and absorb in UV) but show high stability in aqueous electrolyte, e.g.: TiO_2, WO_3, $SrTiO_3$, $BaTiO_3$, SnO_2, ZnO while low band gap materials are good harvesters but show poor stability in aqueous electrolyte,
e.g.: Si, GaAs, InP, CdTe, CdSe, CuO.

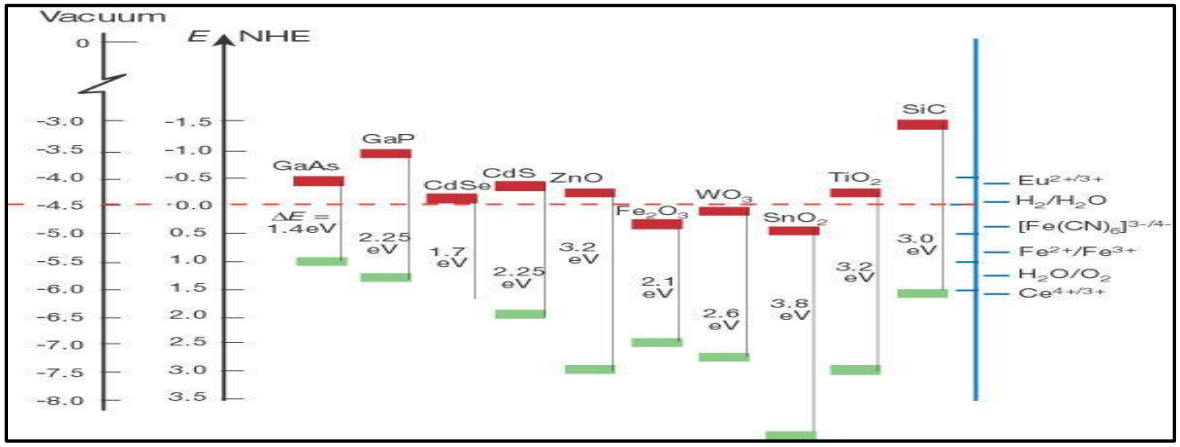

Fig.3. Band positions of several semiconductors in contact with aqueous electrolyte at pH 1[8].

1.7 Strategies Adopted to Improve Photoelectrochemical Response

It is a well known fact that there are various methods which are known to enhance the photoelectrochemical response. Some of the well studied methods are summarized below:

1. **Nanomaterials:**

Photoelectrodes with semiconductors like CdS, Bi_2S_3, Sb_2S_3, WO_3, ZnO, Fe_2O_3, and, more commonly, TiO_2 have been explored and offer potential advantages over their bulk counterparts. There are several reasons because of which nanostructured semiconductor shows enhanced response[32]:

- Nanostructured photoelectrodes provides an extremely large surface area for the redox reactions to take place.
- Distance for photogenerated holes to diffuse to the photoanode/electrolyte interface reduces as the size of nanomaterials decreases for the oxidation of water.
- By varying the size of semiconductor nanocrystals, band gap can be tuned to increase the light absorption in the solar spectrum.

2. **Doping:**

Impurity doping raises the number of charge carriers and/or increases the carrier mobility and thereby improves electrical conduction. Doping by higher- or lower-valent ions is known to produce mixed valence states which in turn influence the PEC response of semiconductor[1].
1% Rh in $SrTiO_3$ was found to possess intense absorption bands in the visible light region due to the transition from the electron donor level formed by Rh ions to the conduction band composed of Ti 3d orbitals of $SrTiO_3$[33]. Carbon-doped nanostructured TiO_2 has lowered the band gap of semiconductor and showed enhanced photoresponse[34]. Pt-Doped[35] and Al- Doped[37] α-Fe_2O_3 , N-Doped ZnO nanowires[36] showed an improvement in photoelectrochemical performance.

3. **Choice of Electrolytes:**

Composition and pH of electrolyte play an important role as these affect onset potential and flatband potential of the semiconductor electrode in PEC cells and thus the PEC response. Proper band-edge matching of the semiconductor with the redox level of water increases the rate of transfer of charge carriers at the junction. Positions of the conduction and valence bands of semiconductors show pH dependence. An increase in pH results in a shift in the conduction- and valence-band positions to more cathodic potentials by 59mV per unit pH at 25^o C following Nernstian behavior. An aqueous solution of electrolyte more generally used is of either acid or alkali which affects the PEC response[1]. Buffer of 0.1M KI and 0.01M K_2HPO_4/KH_2PO_4 (pH 6.8) in water were also employed as electrolyte to study the PEC response of nanorod thin films of α-Fe_2O_3[1a.] An aqueous solution of 0.2M $Na_2B_2O_4$, 0.2M $Na_2B_4O_7$, 0.14M H_2SO_4 and 0.3M

Na_2SO_4 were also used as the supporting electrolyte in some studies[1b-1c]. Anodized nanoporous iron(III) oxide was studied in an electrolyte containing 0.5M H_2O_2 (50%) and 1M NaOH (50%) which revealed that addition of H_2O_2 to the electrolyte greatly enhance the PEC response[1d].

4. Porosity:

Photocurrent obtained from semiconductor electrode in PEC cell are found to be influenced by the porosity of the film. The semiconductor electrode/electrolyte junction is the site of electrochemical reactions which is responsible for PEC splitting of water. Porosity of semiconductor decides the overall surface area of contact between electrodes and electrolytes. More is porosity, more is the contact area, which in turn is expected to improve the PEC response of the material, but very high porosity are also known to cause high resistance[1].
Nanoporous α-Fe_2O_3 prepared by potentiometric anodization and it was observed that anodization conditions and electrolytic composition determine the pore diameter, which ranged between 50- 250 nm and 300- 600 nm in length, with a pore depth of approx. 500 nm[1d].

5. **Layered Structures:**

Combination of small- and large-bandgap material deposited one over the other may absorb the full solar spectrum more efficiently. Better and efficient separation of photogenerated electrons and holes is possible when energy band edges matches at the junction. The electron transfer between the two semiconductors can enhance charge separation and inhibit recombination rate of charge carriers[1].
Bilayered photoelectrode α-Fe_2O_3/TiO_2 system incorporating TiO_2 thin films prepared by the sol-gel technique over a spray-pyrolytically deposited thin film of α-Fe_2O_3 has been studied and photoresponse obtained was much larger than those of the single-material electrodes[1e].

6. Swift Heavy Ion Irradiation:

Swift heavy ion (SHI) irradiation plays a vital role by modifying the properties of films, foils and surfaces of bulk solids as these penetrates deep into the materials and produces a long and narrow disordered zone along its trajectory.

SHI irradiation in semiconductors have been investigated for semiconductors like Fe_2O_3, CuO, $BaTiO_3$, $SrTiO_3$, TiO_2 and ZnO and showed enhanced photoresponse at optimum fluence which was attributed to[21-30]:

- Lowest resistivity
- Maximum flatband potential
- Improved optical absorption capability
- Increased roughness

- Decrease in the average grain diameter

7. Dye Sensitization:

Dye sensitized semiconductors has been investigated for better use of solar light in field of photovoltaics, photocatalysis and photoelectrochemistry. Its success depends upon the collection of photogenerated electrons at external circuit without any disturbance. For efficient electron transfer, the electrode should possess- good transport property in the semiconductor matrix, fast recovery of electron to the oxidized dye and good electron separation. But instability of dye sensitized photoelectrodes limits their use in PEC water splitting[31].

Iridium oxide nanoparticles were stabilized by a heteroleptic ruthenium tris(bipyridyl) dye which were used as sensitizers in photoelectrochemical cells consisting of a nanocrystalline anatase anode and a Pt cathode. The dye coordinated the $IrO_2 \cdot nH_2O$ nanoparticles through a malonate group and the porous TiO_2 electrode through phosphonate groups. Under visible illumination ($\lambda > 410$ nm) oxygen and hydrogen was generated at small applied voltage[38].

1.7 Effect of Plasmons for Photoelectrochemical Water Splitting

P**lasmon** can be defined as quantum of plasma oscillation. Plasmon is a quasiparticle resulting from the quantization of plasma oscillations similar to photons which result from quantization of electromagnetic vibrations. Plasmons that are confined to surfaces and that interact strongly with light resulting in a polariton are referred to as surface plasmons[39].

Most outstanding optical property of metallic nanostructures is surface plasmon resonance (SPR). It consists of a collective oscillation of conduction electrons excited by the electromagnetic field of light. In metallic nanoparticles, electric field produced by electron oscillations will be much higher than the incident light. With decrease in the size (few nanometers) of metallic particles, their optical properties get dramatically modified by appearance of SPR and their behavior is entirely different from the bulk counterpart. They show the property to concentrate and amplify the electric field of light which can be explored to increase the efficiency of photoenergetic processes[40].

It is proposed to utilize the above mentioned properties of plasmons in the photoelectrochemical studies with respect to change in the properties of semiconductor material involved.

To get enhanced photoelectrochemical performance by exploiting localized surface plasmon effects in a target system, following points must be considered[9]:

- Determine whether semiconductor has inadequate light absorption and can therefore benefit from plasmon enhancement.
- Resonant coupling between the plasmonic metal nanoparticles and semiconductor must be considered to ensure that energy transfer between the metal and semiconductor.

- Maximum achievable photovoltage is determined by the work function of the metal and the corresponding Schottky barrier formed by the semiconductor metal nanoparticle interface.

Introduction of noble metal nanoparticles to the semiconductor leads to improved photoelectrochemical performance because of the following reasons:

- Localized photon absorption at the semiconductor surface, and therefore in the space charge layer[9].
- Quasi-Fermi level of the composite shift to more negative potentials[10].
- The noble metal NPs can act as a sink for photoinduced charge carriers, promoting interfacial charge-transfer processes in composite systems[11].

1.8. Effect of Swift Heavy Ion Irradiation for Photoelectrochemical Water Splitting[26-28]

Semiconductor materials can also be modified by using energetic ions to induce changes in property and surface characteristics of materials. Swift heavy ion (SHI) irradiation is a unique post-deposition treatment, used to modify structural, optical and optoelectronic properties of thin film samples through the intense interaction of incident ions with the target atoms.

When SHI enters a solid with a velocity comparable with the Bohr velocity of electron (2.18 x 10^8 m/s), it imparts its energy via two processes:

1. **Nuclear energy loss** :- Direct transfer of energy to target atoms through elastic collisions
   - cause atomic displacements
2. **Electronic energy loss** (electronic excitation):- Occurs between the incoming ions and electrons of the target atoms due to the inelastic collision.

SHI irradiation can be used to modify the crystallographic, optical, electrical and morphological properties of materials.
Therefore, irradiation can lead to a controlled introduction of defect states in the material system, it has been and being beneficially used to control the material properties.

SHI irradiation of nanocrystalline materials may leads to following modifications:

- Creation of amorphous band in the lattice
- Development of subnanoparticles on account of grain fragmentation due to confinement of energy in the small volume of nanoparticles during swift heavy ion irradiation
- Impurity segregation on grain boundaries.

Such modifications, occurring at atomic and grain level, would lead to alteration in properties viz. bandgap, resistance and structural defects, which are definitely expected to modify the photoelectrochemical response of the material.

2. Literature Survey

The work in the area of water splitting for H_2 generation was pioneered by *Fujishima* and *Honda* in 1972.

People are working in the area of metal oxide with surface plasmon resonance (SPR) for water splitting for some years. Review of the work done in recent years giving good response is given below:

- Thimsen[9] *et al* prepared Au/ Fe_2O_3 by spray pyrolysis. SEM study was done to see the size distribution. UV-Vis spectra shows that Au nanoparticles exhibited plasmonic behavior and showed an increase in the UV-Vis light absorbance. In embedded configuration no enhancement in spectral response was observed due to poor spectral overlap between the plasmonic metal nanoparticle and semiconductor while in surface configuration, enhancement in the spectral response of the electrode was observed and thereby in water splitting efficiency due to the plasmonic absorption and subsequent energy transfer to the semiconductor.

- Takai[10] *et al* prepared Ag/ TiO_2 nanocomposite by photocatalytic deposition of Ag on TiO_2 NPs. A current of 0.056mA/cm^2 at 0V vs (Ag/AgCl) was obtained. Electrons are stored in the TiO_2/Ag composite (more charge accumulation in semiconductor) which assisted in maintaining a more negative Fermi level than pristine TiO_2. Photocurrent of TiO_2/Ag was about 2 times higher than that of pristine TiO_2.

- Naseri[11] *et al* prepared Au/TiO_2 Nanocomposite by Sol-gel method. Formation of gold nanoparticles was confirmed by optical density spectra. Bandgap energy of the Au: TiO_2 films were found to decrease with increasing Au concentration. X-ray diffractometry showed the formation of gold nanocrystals in the anatase TiO_2 nanocrystalline thin films. X-ray photoelectron spectroscopy revealed the presence of gold in the metallic state and the formation of TiO_2 is stoichiometric. The photocurrent of 0.35mA/cm^2 was obtained at 0.5V vs Ag/AgCl. Au NPs (5 mol%) in TiO_2 films showed enhanced photoresponse (2 times higher than plain TiO_2) at increased annealing temperature due to complete formation of Au NPs. Photoresponse increased due to increase in the conductivity, visible light absorption and improvement of charge transfer.

- Liu[12] *et al* prepared Au/TiO_2 by electrochemical anodization. 0.3 μA photocurrent was obtained at 633nm. Under visible light photocurrent was 5 x and 66 x enhanced at wavelengths 532 nm and 633 nm respectively. Near-field optical enhancement increases the e^-/h^+ pair generation rate at the surface of the TiO_2, thus increases the amount of photogenerated charge contributing to catalysis. Intense local fields are also produced by the surface plasmons which couple light efficiently to the surface of the TiO_2.

- Chen[13] *et al* prepared Au/ZnO nanorods by hydrothermal method. 1.3mA/cm^2 photocurrent was obtained at 1.0V vs (Ag/AgCl). Scanning electron microscopic (SEM) images showed the growth of dense and vertically aligned ZnO nanorods on the FTO substrate. Evidence of Au nanoparticles attached to its surface was confirmed by TEM image. Hot electrons generated by Au are injected into the conduction band of the ZnO,

while the plasmon-induced electromagnetic field creates vacancies in the conduction band of the surface of ZnO, promoting the separation of photogenerated electrons and holes. Photocurrent density in Au/ZnO nanorods was double that of pristine ZnO nanowires of same thickness.

- Ingram[14] *et al* prepared Ag/N-TiO_2 (TiO_2 anatase annealing in presence of NH_3, Pylol process to prepare Ag nanocubes). Average photon path length in the composites increased due to scattering of photons by Ag causing an increased rate of e^-/h^+ pair formation in N-TiO_2. Intense electric fields are encountered by semiconductor due to Ag in its proximity, resulting in rapid formation of e^-/h^+ pair. Increase in the visible-light photocurrent was observed by a factor of ~10 on addition of plasmonic Ag nanoparticles to N-TiO_2.

Review of the work done in recent years on the different metal oxide giving good response for water splitting with highly enhanced response is given below:

- Zhang[15] et al prepared carbon layer protected Cu_2O nanowire arrays by electrochemical anodization. Transmission electron microscope (TEM) and scanning electron microscopy (SEM) were used to study morphology of nanowire arrays. The crystalline structure of the samples was analyzed by X-ray diffraction (XRD) and chemical compositions and status were analyzed by X-ray photoelectron spectroscopy (XPS). 3.95mA/ cm^2 photocurrent was obtained at 0V vs RHE. Good conductivity of the carbon layer on the Cu_2O nanowire surface facilitated the electron transfer from Cu_2O to the electrolyte resulting in an reduced charge transfer resistance. The problem of photocorrosion problem of semiconductors can be combated by carbon layer protection.

- Wang[16] *et al* prepared double sided CdS and CdSe quantum dot co-sensitized ZnO nanowire arrays by hydrothermal method and chemical bath deposition. Structural properties were investigated by using electron microscopy and powder X-ray diffraction (PXRD) studies. Growth of dense and vertically aligned ZnO NWs on both sides of the ITO substrate, with typical wire diameter of ~100-150 nm and wire length of ~2 μm was revealed by scanning electron microscopy (SEM) images. TEM images verified that individual ZnO NWs were covered with nanoparticle aggregates after QD sensitization. Photocurrent of 12mA/cm^2 at 0.4V vs (Ag/AgCl). Photoanode showed strong absorption in nearly the entire visible spectrum up to 650 nm. Incident-photon-to-current-conversion efficiency (IPCE) reached ~45% at 0 V vs Ag/AgCl due to the Fermi level alignment between CdS and CdSe.

- Tilley[17] *et al* deposited IrO_2 on Fe_2O_3. IrO_2 NP deposition was done by electrophoresis. Photocurrent of 3mA/cm^2 was obtained at 1.23V vs RHE. X-ray photoelectron spectroscopy (XPS) revealed a surface concentration of iridium of 1.0 at. %. Slight reduction in photocurrent over 200 seconds at +1.23 V versus RHE was observed

indicating IrO_2 particles are not stably adhered to the hematite and detach from the surface.

- Seol[18] *et al* prepared $IrO_x \cdot nH_2O$ modified CdSe/CdS quantum dot cosensitized ZnO nanowire by chemical bath deposition. Photocurrent of 8.3 mA/ cm^2 was obtained at 0 V vs RHE. Scanning electron microscopy (SEM) was used to study the size and morphology of the prepared nanowires and it showed uniform distribution of $IrO_x \cdot nH_2O$. The electron energy loss spectroscopy (EELS) elemental mapping and energy-dispersive X-ray spectroscopy (EDS) line scanning showed that $IrO_x \cdot nH2O$ nanoparticles (ca. 1.7 at%) have fairly uniform distribution without any aggregates on the entire surface of the CdSe/CdS/ZnO nanowire. Stable photocurrent was obtained with $IrO_x \cdot nH_2O$ modification as it scavenges holes and retards electron- hole recombination as well as hole-induced anodic corrosion of quantum dots.

- Kang[19] *et al* prepared reduced TiO_2 nanotube arrays by electrochemical anodization. Photocurrent of 0.73mA/cm^2 was obtained at 1.23V vs RHE. $NaBH_4$ treatment of TiO_2 nanotube arrays created surface oxygen vacancy, increasing the donor density of TiO_2 NTAs by 2 fold, decreasing surface recombination centers and favoring charge transfer rate, creating localized states in the band gap thereby extending optical absorption to the visible region. Field emission-SEM showed well aligned nano tubes vertically oriented from the Ti foil substrate which promotes directional charge transport. Electron paramagnetic resonance (EPR) spectra confirmed the presence of oxygen vacancy on the surface and inner of TiO_2.

- Wang[20] *et al* prepared vertically aligned ZnO/CdTe core shell nanocable arrays by electrochemical deposition. Photocurrent of 5.9mA/cm^2 was obtained at 0V vs SCE. Field-emission scanning electron microscope (SEM) images showed ZnO nanorods arrays on an ITO substrate with hexagonal cross section. XRD showed that ZnO is formed in quartzite phase. EDX spectrum confirms that the nanocable is composed of Zn, O, Cd, and Te and that both the Zn/O and Cd/Te ratios are close to 1.Type II band alignment of CdTe with ZnO allows the effective injection of photogenerated electrons from CdTe into ZnO. 30-fold increase in the current density was observed when the measurement performed in the dark.

Work done from the research group at DEI on the study of semiconductors modified by SHI irradiations for enhanced PEC response are summarized below:

Author	**Material/ Method/ Ion**	**Applied Bias(V/SCE)/ Photoresponse (mA/cm^2)**	**Remarks**
Chaudhary[21] *et al* 2006	2% Cr- Fe_2O_3 Spray Pyrolysis	**Bias:** 0.95	• Efficient absorption of photons (Decrease in Eg). ✓ *This response is obtained at fluence of 10^{12} ions/cm^2.*
	Ion/Energy: 170MeV Au^{13+}	**Unirradiated:** 0.5 **Irradiated:** 2.5	
Singh[22] *et al* 2009	Fe_2O_3, Spray Pyrolysis	**Bias:** 0.95	• Reduction in grain size • Flatband potential and Donor density were maximum at this fluence. • Increase in the donor density and decrease in resistivity was attributed to the partial transformation of α-Fe_2O_3 to Fe_3O_4 phase. ✓ *This response was obtained at fluence of 10^{13} ions/cm^2*
	Ion/Energy: 120MeV Ag^{9+}	**Unirradiated:** 0.06 **Irradiated:** 0.32	
Singh[23] *et al* 2008	Fe_2O_3, Spray Pyrolysis	**Bias:** 0.95	• Flatband potential were maximum at this fluence ✓ *This response was obtained at fluence of 2 x 10^{13} ions/cm^2*
	Ion/Energy: 100MeV Si^{7+}	**Unirradiated:** 0.06 **Irradiated:** 0.36	
Kumar[24] *et al* 2011	Fe_2O_3, Electrodeposition	**Bias:** 0.75	• Decrease in the resistivity, increase in donor density and increase in flatband potential at this fluence ✓ *This response was obtained at fluence of* 5x10^{12}*ions/cm^2*
	Ion/Energy: 100 MeV Si^{8+}	**Unirradiated:** 1.6 **Irradiated:** 3.0	

Chaudhary[25] *et al* 2004	CuO Spray Pyrolysis	**Bias:** 0.3	• Photoelectrochemical response *decreased*, attributed to creation of greater number of kink sites/dislocations, acting as recombination centers for photogenerated charge carriers. ✓ *This response was obtained at fluence of 10^{13} ions/cm^2*
	Ion/Energy:170 MeVAu^{13+}	**Unirradiated:**2.45	
		Irradiated: 1.04	
Solanki[26] *et al* 2013	$BaTiO_3$ Sol-gel	**Bias:** 0.4	• Maximum negative value of the flatband potential and donor density and lowest resistivity at this fluence. ✓ *This response was obtained at fluence of 5 x 10^{11} ions/cm^2*
	Ion/Energy:100 MeVSi^{8+}	**Unirradiated:** 0.1	
		Irradiated: 0.7	
Solanki[27] *et al* 2013	$BaTiO_3$ Sol-gel	**Bias:** 0.4	• Improved optical absorption capability, increased roughness and efficient separation of charge carriers • Maximum flatband potential and donor density. ✓ *This response was obtained at fluence of 10^{11} ions/cm^2*
	Ion/Energy:120 MeVAg^{9+}	**Unirradiated:** 0.1	
		Irradiated: 1.78	
Solanki[28] *et al* 2011	$SrTiO_3$ Sol-gel	**Bias:** 0.0	• Decrease in the average grain diameter • Reduction in bandgap • Increase in roughness. ✓ *This response was obtained at fluence of : 3x10^{12} ions/cm^2*
	Ion/Energy:120 MeVAg^{9+}	**Unirradiated:** 0.05	
		Irradiated: 0.16	
Singh[29] *et al* 2010	TiO_2 Sol-gel	**Bias:** 0.0	• Decrease in the average grain diameter • Maximum flatband potential and charge carrier density. ✓ *This response was obtained at fluence of : 5x10^{11}ions/cm^2.*
	Ion/Energy:120 MeVAg^{9+}	**Unirradiated:** 0.09	
		Irradiated: 0.76	

Gupta[30] *et al* 2009	ZnO Sol-gel	**Bias:** 0.0	• Lowest resistivity (higher carrier mobility) for sample sintered at 500^0C, attributing increase in photocurrent. ✓ *This response was obtained at fluence of : $3x10^{12}$ ions/cm^2*
	Ion/Energy:120 MeVAg^{9+}	**Unirradiated:** 0.001	
		Irradiated: 0.0011	

All the above obtained results were supported by the XRD, AFM, SEM, XPS analysis, ERDA analysis, UV-Visible spectroscopy, Raman spectroscopy. Highest photocurrent was obtainable at optimum fluence and higher fluence results in amorphization of the sample which decreases the photoresponse.

3. Proposed Study

The proposed work deals with the effect of ion beams on nanostructured oxide thin films embedded/coated with the noble metal particle with aim to study the modification of metal oxide films for photoelectrochemical water splitting for generation of hydrogen.

Some of metal oxides which have shown good response in PEC splitting of water will be studied e.g., ZnO, CuO and TiO_2. These nanostructured metal oxides will be synthesized by sol-gel method and spray pyrolysis. The noble metal nanoparticles over the films will be deposited by RF sputtering and magnetron sputtering. The metal nanoparticles deposition will be done in between the layers and over the surface. Then PEC study will be carried out on the prepared samples. The best responding samples will be irradiated with different energy ion beams to see the altered response of the samples for PEC water splitting.

4. Objectives of Study

The proposed work plan will have following objectives:

1. Preparation of nanostructured metal oxides (CuO, ZnO, TiO_2) by :
✓ Spray Pyrolysis
✓ Sol-gel

2. Embedding of noble metal particles in between layers and at the surface either by RF sputtering or magnetron sputtering.

3. Characterization of thin films of metal oxide nanoparticles will be done by:
✓ XRD: To observe the formation of different phases and to estimate the average grain/particle size using Scherrer's calculations.
✓ SEM and AFM: to observe the surface morphology of the films.

- ✓ Band-gap (UV- Visible Spectroscopy)

Besides, the samples would also be characterized for resistivity, thickness and n-type and p- type nature of semiconductor.

4. Study of photoelectrochemical behavior of thin films of nanostructured metal oxides both in dark and under illumination at different electrolytic conditions (pH, nature of electrolyte etc.) will be done for all samples.

5. Irradiation of the samples with different energy beams of Ag and O with different fluences will be done for samples giving good response in PEC in order to study modified properties with respect to PEC response.

5. Experimental Plan

1. Preparation of samples

The study involves sample preparation of various noble metal nanoparticles incorporated thin films of ZnO, CuO, TiO_2 .The thin film will be prepared by sol gel and spray pyrolysis methods. After then for incorporation of noble metal nanoparticles will be done by sputtering either by magnetron or RF sputtering available at IUAC, New Delhi. In this process atoms are ejected from a solid target material due to bombardment of the target by energetic particles.

2. Characterization of thin films

Structure and Surface Morphology:

Structural analysis of the samples would be performed by X-ray diffraction technique to check the polycrystallinity of the compound formed, and to confirm the formation of desired phase.

For determining surface morphologies, such as, grain size (particle size), grain structure and surface roughness of the material, SEM (scanning electron microscopy) analysis would be used.

XRD, SEM, AFM would be done at the Dayalbagh Educational Institute, Agra.

Particle size analysis:

The size of the particles, within the range, nanodimensions, plays a very important role in modifying the properties of the materials. Hence, this measurement is expected to be a crucial part of the proposed study. The particle size would also be determined for the XRD data using Scherrer's equation.

Film thickness:

Aplha step D-Tencor T120 (surface profilometer) available at Dayalbagh Educational Institute, Agra will be used to measure film thickness.

Bandgap:

Using *Tauc* plots, E_g will be determined by plotting $(\alpha h\nu)^{1/2}$ vs. $h\nu$ using the equation below:

$$\text{Absorption coefficient, } \alpha = A\,(h\nu - E_g)^{1/2}$$

The above calculation will be done by UV-Vis spectrophotometer (shimadzu, UV-2450) in Dayalbagh Educational Institute, Agra.

Resistivity measurement:

Transverse resistance and, thus, resistivity of the sample will be measured by resistance meter. Additionally current voltage characteristics would also be used for resistance measurement. For this purpose a large contact would be made on one side of sample while on the reverse side a small pressure contact would be used.

Mott-Schottky plot*:*

An LCR meter would be employed to measure capacitance (C) at semiconductor electrolyte junction. $1/C^2$ versus electrode voltage plot will give band bending, flatband potential and donor/acceptor densities with the help of following Mott-Schottky equation.

$$\frac{1}{C^2} = \left(\frac{2}{q\varepsilon_o \varepsilon N_D}\right)\left(V_{app} - V_{FB} - \frac{kT}{q}\right)$$

Where ε_o is the permittivity of the vacuum, N_D is the donor density, V_{app} is the applied potential, ε is the dielectric constant of the semiconductor, kT/q is the temperature dependent term.
Nature of semiconductor can be known from the slope as:

+ve Slope- n- type
-ve Slope- p- type

3. Photo-electrochemical studies:

Photo-electrochemical measurements would be done for unirradiated semiconductor samples (thin films), as photosensitive working electrode, in conjunction with platinum counter electrode and saturated calomel electrode (SCE, as reference electrode), at varying electrolyte conditions. Nature and concentration of the electrolyte and electrolyte- pHs would also be varied in order to optimize the conditions of H_2 evolution.

I-V characteristics of PEC cell would be studied, both under darkness and illumination. Light source, to be employed for this purpose, would be a 300W Solar Simulator (Newport, earlier Oriel.

By observing the I-V plots, onset voltage for photocurrent would be determined, and based on these measurements the performance of PEC cell would be evaluated.

Efforts would also be made to collect the evolved gases from PEC cell and pass them through alkaline pyrogallol solution at 0-5°C to remove oxygen. Rest of the gas (largely hydrogen) would then be collected in a gas measuring tube, slowly, by displacing the water. The collected gas would be analyzed for hydrogen by employing a gas chromatograph and efficiency of hydrogen production would be calculated.

4. Irradiation of Thin Films

Thin films giving good response for water splitting will then be irradiated by Ag and O at energies between 100-120 MeV with different fluence.

Photoelectrochemical response of the irradiated films will again be taken to compare the results before and after irradiation.

6. References

1. Vayssieres, L.; On Solar Hydrogen & Nanotechnology; **2009** , John Wiley & Sons (Asia) Pte Ltd

   a. Beermann, N.,Vayssieres, L., Lindquist, S. E., and Haqfeldt, A.; Photoelectrochemical studies of oriented nanorod thin films of hematite, *J. of the Electrochemical Soc.*, **2000,** 147, 2456-2461.

   b. Watanabe, A. and Kozuka, H.; Photoanodic properties of sol gel derived Fe_2O_3 thin films containing dispersed gold and silver particles, *J. of Phys. Chem. B*, **2003,** 107, 12713-12720.

   c. Miyake, H. and Kozuka, H.; Photoelectrochemical properties of Fe_2O_3 Nb_2O_5 films prepared by sol gel, *J. of Phys. Chem. B* , **2005,** 109, 17951-17956.

   d. Prakasam, H.E., Varghese, O.K., Paulose, M.; Synthesis and photoelectrochemical properties of nanoporous iron (III) oxide by potentiostatic anodization, *Nanotechnology*, **2006**, 17, 4285- 4291.

   e. Satsangi,V.R., Singh, A.P., Johri, P.; Bilayered photoelectrode for solar hydrogen production system; *Proceedings of XXXI National Systems Conference (CD), Manipal, Karnatika, India*, Dec 14 15, **2007**.

2. http://www.hai.org.in/home.html

3. Bak, T., Nowotny, J., Rekas, M., Sorrell, C.C.; Photo-electrochemical hydrogen generation from water using solar energy; *Int. J. of Hydrogen Energy*; **2002**, 27, 991 – 1022.

4. Chen, Z., Jaramillo, T. F., Deutsch, T. G., Shwarsctein, A. K., Forman, A. J., Gaillard, N., Garland, R. Takanabe, K., Heske, C. Sunkara, M., McFarland, E. W., Domen, K., Miller, E. L., Turner, J. A., Dinh, H. N.; Accelerating materials development for photoelectrochemical hydrogen production: Standards for methods, definitions, and reporting protocols; *J. Mater. Res.*; **2010**, 25 (1), 3-16.

5. Nozik, A. J., Miller, J. R.; Introduction to Solar Photon Conversion; *Chem. Rev.*; **2010**, 110(11), 6443–6445.

6. www.hydrogen.energy.go

7. Choudhary, S., Upadhyay, S., Kumar, P., Singh, N., Satsangi, V. R., Shrivastav, R., Dass, S.; Nanostructured bilayered thin films in photoelectrochemical water splitting- A review; *Int. J. of Hydrogen Energy*; **2012**, 37(24), 18713-18730.

8. Grätzel,M., Photoelectrochemical cells; *Nature*; **2001**, 414

9. Thimsen E., Formal F. Le, Gratzel, M., Warren, S.C.; Influence of Plasmonic Au Nanoparticles on the Photoactivity of Fe_2O_3 Electrodes for Water Splitting; *Nano Lett.;* **2011**, 11, 35–43.

10. Takai, A. and Kamat, P.V.; Capture, Store, and Discharge: Shuttling Photogenerated Electrons across TiO_2/Silver Interface ; *ACS Nano*, **2011**, 5(9), 7369–7376.

11. Naseri, N., Amiri, M., and Moshfegh, A. Z.; Visible photoenhanced current–voltage characteristics of Au:TiO_2 nanocomposite thin films as photoanodes; *J. Phys. D: Appl. Phys*, **2010**, 43, 105405.

12. Liu,Z., Hou, W., Pavaskar, P., Aykol, M., Cronin, S.B.; Plasmon Resonant Enhancement of Photocatalytic Water Splitting Under Visible Illumination; *Nano Lett*, **2011**, 11, 1111–1116.

13. Chen, H. M., Chen, C.K.,Chen, C., Cheng, L., ChiehWu, P., Cheng, B.H., Ho, Y.Z., Tseng, M.L., Hsu, Y., Chan, T., Lee, J., Liu, R., Tsai , D.P.;Plasmon Inducing Effects for Enhanced Photoelectrochemical Water Splitting: X- ray Absorption Approach to Electronic Structures; *ACS nano*, **2012**, 6 (8), 7362–7372.

14. Ingram, D. B., Linic, S.; Water Splitting on Composite Plasmonic-Metal/Semiconductor Photoelectrodes: Evidence for Selective Plasmon-Induced Formation of Charge Carriers near the Semiconductor Surface; *J. Am. Chem. Soc*, **2011**, 133, 5202–5205

15. Zhang, Z., Dua, R., Zhang, L., Zhu, H., Zhang, H., Wang,P.; Carbon-Layer-Protected Cuprous Oxide Nanowire Arrays for Efficient Water Reduction; *ACS Nano.*

16. Wang, G., Yang, X., Qian, F., Zhang, J. Z., and Li, Y.; Double-Sided CdS and CdSe Quantum Dot Co-Sensitized ZnO Nanowire Arrays for Photoelectrochemical Hydrogen Generation*; Nano Lett.*,**2010,** *10*, 1088–1092.

17. Tilley, S.D., Cornuz, M., Sivula, K., and Gratzel, M.; Light-Induced Water Splitting with Hematite: Improved Nanostructure and Iridium Oxide Catalysis; *Angew. Chem*. **2010**, 122, 6549 –6552.

18. Seol,M., Jang, J., Cho, S., Lee, J.S., Yong, K.; Highly Efficient and Stable Cadmium Chalcogenide Quantum Dot/ ZnO Nanowires for Photoelectrochemical Hydrogen Generation; *Chem. Mater.* **2013**, 25, 184−189.

19. Kang, Q., Cao, J., Zhang, Y., Liu, L., Xu, H., Ye, J.; Reduced TiO_2 Nanotube Arrays for Photoelectrochemical Water Splitting; *J. of Mat. Chem. A*, DOI: 10.1039.

20. Wang, X., Zhu, H., Xu, Y., Wang, H.,Tao, Y., Hark, S.,Xiao, X., Li, Q.; Aligned ZnO/CdTe Core/Shell Nanocable Arrays on Indium Tin Oxide: Synthesis and Photoelectrochemical Properties, *ACS Nano*, **2010**, 4(6),3302-3308.

21. Chaudhary, Y.S., Khan, S.A., Tripathi, C., Shrivastav R., Satsangi V. R., and Dass, S.; A study on 170 MeV Au^{13+} irradiated nanostructured metal oxide (Fe_2O_3 and CuO) thin films for PEC applications; *Nucl. Instr. and Meth. B*, **2006**, 244(1), 128-131.

22. Singh, A.P., Kumari**, S.,** Shrivastav,R., Dass,S., Satsangi, V.R. ; Improved Photoelectrochemical response in Hematite by high energy Ag^{9+} ions irradiation", *J. Phys. D: Applied Physics*, **2009**, 42, 085303.

23. Singh, A.P, Tripathi,A., Shrivastav,R., Dass,S., Satsangi, V.R. ; New Benchmark to Improve the Photoelectrochemical Properties of Hematite; *Proc. of SPIE* , **2008**, 7044, 70440H-1.

24. Kumar, P., Sharma P., Solanki, A., Tripathi,A., Deva D., Shrivastav, R., Dass, S., Satsangi, V.R.; Photoelectrochemical generation of hydrogen using 100 Mev Si^{8+} ion irradiated electrodeposited iron oxide thin films; *Int. J. Hydrogen Energy*, **2012**, 4, 3626-3632.

25. Chaudhary, Y.S., Khan, S.A., Shrivastav, R., Satsangi, V.R., Prakash,S., Avasthi , D.K., Dass, S.; A study on 170 MeV Au^{13+} irradiation induced modifications in structural and photoelectrochemical behavior of nanostructured CuO thin films; *Nuc. Inst. and Methods in Physics Res. B*, **2004**, 225, 291–296.

26. Solanki, A., Choudhary, S., Satsangi, V.R., Shrivastav, R., Dass, S.; Enhanced photoelectrochemical properties of 100 MeV Si^{8+} ion irradiated barium titanate thin films, *J. of Alloys and Compounds*, **2013**, 561, 114–120.

27. Solanki, A., Shrivastava, J., Upadhyay, S.,Choudhary, S., Sharma, V.,Sharma, P., Kumar, P., Kumar, Praveen, Ehrman, S., Satsangi, V.R., Shrivastav, R., Dass, S.; Modified structural, morphological and photoelectrochemical properties of 120 MeV Ag^{9+} ion irradiated BaTiO3 thin films *Current Applied Physics*, **2013,** 13(2), 344-350.

28. Solanki, A., Shrivastava, J., Upadhyay, S., Sharma, V., Sharma P., Kumar, P., Praveen Kumar, Gaskell, K., Satsangi, V.R., Shrivastav,R., Dass,S.; A Case Study of $SrTiO_3$ Thin Films Irradiated By 120 Mev Ag^{9+} Ion; *Int. J. Hydrogen Energy*, **2011,** 36, 5236-5245

29. Singh, A.P., Kumari**,** S., Tripathi, A., Singh, F., Gaskell, K.J., Shrivastav, R., Dass, S., Ehrman,S.H., Satsangi, V.R. ; Improved Photoelectrochemical Response of Titanium Dioxide irradiated with 120 MeV Ag^{9+} ion ; *J. of Phys. Chem. C*, **2010,** 114 (1), 622–626.

30. Gupta, M., Shrivastava J., Sharma, V., Solanki, A., Singh, A. P. , Satsangi, V. R., Dass S., Shrivastav, R.; Enhanced Photoelectrochemical Activity of 120 MeV Ag^{9+} Irradiated

Nanostructured Thin Films of ZnO for Solar-Hydrogen Generation via Splitting of Water; *Advanced Materials Research*; **2009**, 67, 95-102.

31. Haque, S.A., Tachibana, Y., Wills, R.L., Moster, J. E., Gratzel, M., Klug, R.D., Durrant, J.R.; Parameters Influencing Charge Recombination Kinetics in Dye-Sensitized Nanocrystalline Titanium Dioxide Films; *J. Phys. Chem. B;* **2000,** 104, 538-542.

32. Li, Y., Zhang, J.Z., Hydrogen generation from photoelectrochemical water splitting based on nanomaterials; *Laser Photonics Rev*., **2010**, 4(4), 517–528.

33. Konta,R., Ishii,T., Kato, H., Kudo, A.; Photocatalytic Activities of Noble Metal Ion Doped $SrTiO_3$ under Visible Light Irradiation; *J. Phys. Chem. B*, **2004**, 108, 8992-8995.

34. Chu, D., Yuan, X., Qin, G., Xu, M., Zheng, P., Lu, J., Zha, L.; Efficient carbon-doped nanostructured TiO2 (anatase) film for photoelectrochemical solar cells; *J Nanopart Res*, **2008**, 10, 357–363.

35. Hu, Y.S., Shwarsctein, A.K, Forman, A. J., Hazen, D., Park, J.N., McFarland, E.W.; Pt-Doped r-Fe2O3 Thin Films Active for Photoelectrochemical Water Splitting, *Chem. Mater.* **2008**, 20, 3803–3805.

36. Yang, X., Wolcott, A., Wang, G., Sobo, A. Fitzmorris, R. C., Qian, F., Zhang, J.Z., Li, Y.;Nitrogen-Doped ZnO Nanowire Arrays for Photoelectrochemical Water Splitting, *Nano Lett.*, **2009,** 9(6), 2331-2336.

37. Shwarsctein,A. K., Huda, M.N., Walsh, A., Yan, Y., Stucky, G.D., Hu, Y.S., Al-Jassim, M, M., McFarland, E. W.; Electrodeposited Aluminum-Doped α-Fe_2O_3 Photoelectrodes:Experiment and Theory, *Chem. Mater.*, **2010**, 22, 510–517.

38. Youngblood, W.J., Lee, S.A., Kobayashi, Y., Hernandez-Pagan, E.A., Hoertz, P.A., Moore, T.A., Moore, A.L., Gust, J., Mallouk, T.E.; Photoassisted Overall Water Splitting in a Visible Light-Absorbing Dye-Sensitized Photoelectrochemical Cell; *J. Am. Chem. Soc.*, **2009**, *131* (3), 926–927.

39. wikipedia.org/wiki/Plasmon

40. Gracia, M.A.; Surface Plasmons in Metallic Nanoparticles: Fundamentals and Applications; *J. Phys. D: Appli. Phys.***, 2011,** 44, 283001.